

Observation of the correlation between the phonon frequency and long-range magnetic ordering on a MnW octacyanide molecule-based magnet

Hiroko Tokoro,^{*a,b} Naotaka Maeda,^a Kenta Imoto,^b Koji Nakabayashi,^b Kouji Chiba,^c
and Shin-ichi Ohkoshi^{*b}

^a *Department of Materials Science, Faculty of Pure and Applied Sciences,
University of Tsukuba, Tsukuba, Japan*

^b *Department of Chemistry, School of Science, The University of Tokyo, Tokyo, Japan*

^c *Material Science Div., MOLSI Inc., Japan*

	Contents	Page
§ 1.	IR spectrum at room temperature.	Fig. S1 S2
§ 2.	Crystallographic data.	Tables S1 S3
§ 3.	Thermogravimetric measurement.	Fig. S2 S4
§ 4.	Powder XRD pattern and Rietveld analysis.	Fig. S3 S5
§ 5.	Magnetic properties.	Fig. S4 S6
§ 6.	IR spectra and peak separation.	Fig. S5 S7
§ 7.	Phonon dispersion obtained by first-principles phonon mode calculations.	Fig. S6 S8
§ 8.	Partial phonon density of states obtained by first-principles phonon mode calculations.	Fig. S7 S9,S10
§ 9.	Far-IR spectra at 12 K and 60 K.	Fig. S8 S11

§ 1. IR spectrum at room temperature.

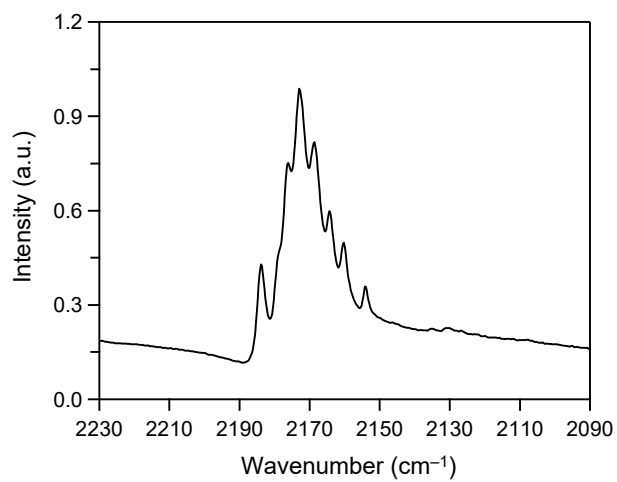


Figure S1. Mid-IR spectrum of **MnW** at room temperature.

§ 2. Crystallographic data.

Table S1. Crystallographic data and structure refinement of **MnW** at room temperature. Crystal structure was solved by direct methods with SHELXS-97 and refined by a full-matrix least-squares method on F^2 with SHELXL-2016/6.^{S1}

Compound	Mn ₃ [W(CN) ₈] ₂ (pyrimidine) ₄ ·6H ₂ O (MnW)
Empirical formula	C ₃₂ H ₂₈ Mn ₃ N ₂₄ O ₆ W ₂
Formula weight	1377.30
Temperature (K)	293(2)
Crystal system	Monoclinic
Space group	$P2_1/n$
a (Å)	7.2319(4)
b (Å)	14.9477(8)
c (Å)	22.4483(13)
β (°)	90.920(6)
V (Å ³)	2426.4(2)
Z	2
ρ_{calc} (g cm ⁻³)	1.885
μ (mm ⁻¹)	5.548
$F(000)$	1318
Crystal size (mm ³)	0.06×0.05×0.02
Radiation	MoK α ($\lambda = 0.71075$)
2θ range for data collection (degrees)	6.090–54.928 –9 < h < 9
Index ranges	–19 < k < 19 –29 < l < 26
Reflections collected	23250
independent reflections	5524 [$R_{\text{int}} = 0.0724$, $R_{\text{sigma}} = 0.0584$]
Data/restraint/parameters	5547 / 0 / 309
GOF on F^2	1.368
Final R indices [$I \geq 2\sigma(I)$]	0.0734 / 0.0932
Final R indices [all data]	0.0901 / 0.0964
Largest diff peak/hole	1.82 / –6.27

S1. Sheldrick, G. M. Crystal structure refinement with SHELXL. *Acta Cryst.* 2015, **C71**, 3–8.

§ 3. Thermogravimetric measurement.

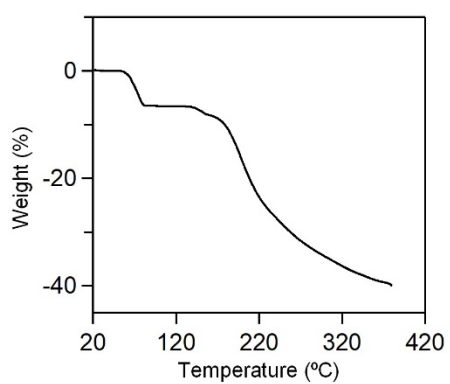


Figure S2. Thermogravimetric measurement of **MnW** under a scan rate of $+2\text{ °C min}^{-1}$. Weight loss is due to the removal of water molecules around 70 °C and pyrimidine molecules from around 160 °C .

§ 4. Powder XRD pattern and Rietveld analysis.

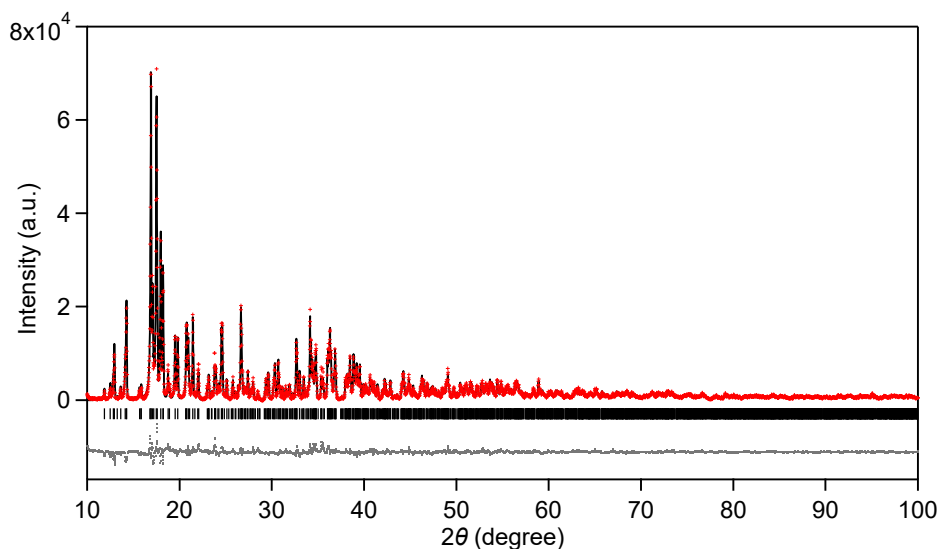


Figure S3. Powder XRD pattern of **MnW** at room temperature and Rietveld analysis. Red dots, black line, grey dots, and black bars represent the observed plots, calculated pattern, their difference, and calculated positions of the Bragg reflections, respectively. Monoclinic ($P2_1/n$) crystal structure with lattice parameters of $a = 7.2348(2) \text{ \AA}$, $b = 14.9552(3) \text{ \AA}$, $c = 22.4502(3) \text{ \AA}$, $\beta = 90.908(1)^\circ$. Values of R_{wp} and S are 4.57% and 3.41, respectively.

*The atomic position is the same as that of a single crystal.

§ 5. Magnetic properties.

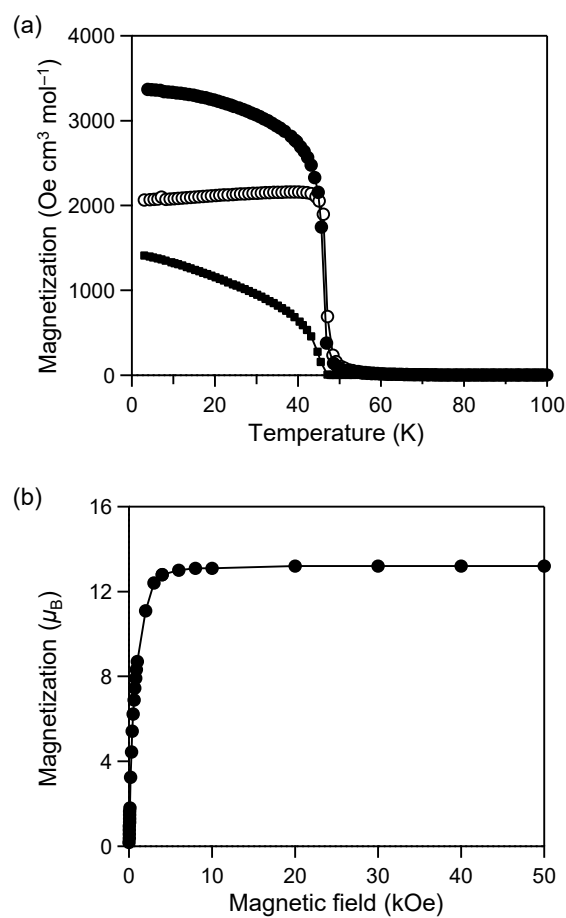


Figure S4. Magnetic properties of **MnW**. (a) Magnetization vs. temperature plots for field-cooled magnetization (FCM) under 20 Oe (black circles), zero field-cooled magnetization (ZFCM) under 20 Oe (open circles), and remnant magnetization (REM) (black squares). (b) Magnetization vs. external magnetic field plot at 2 K.

§ 6. IR spectra and peak separation.

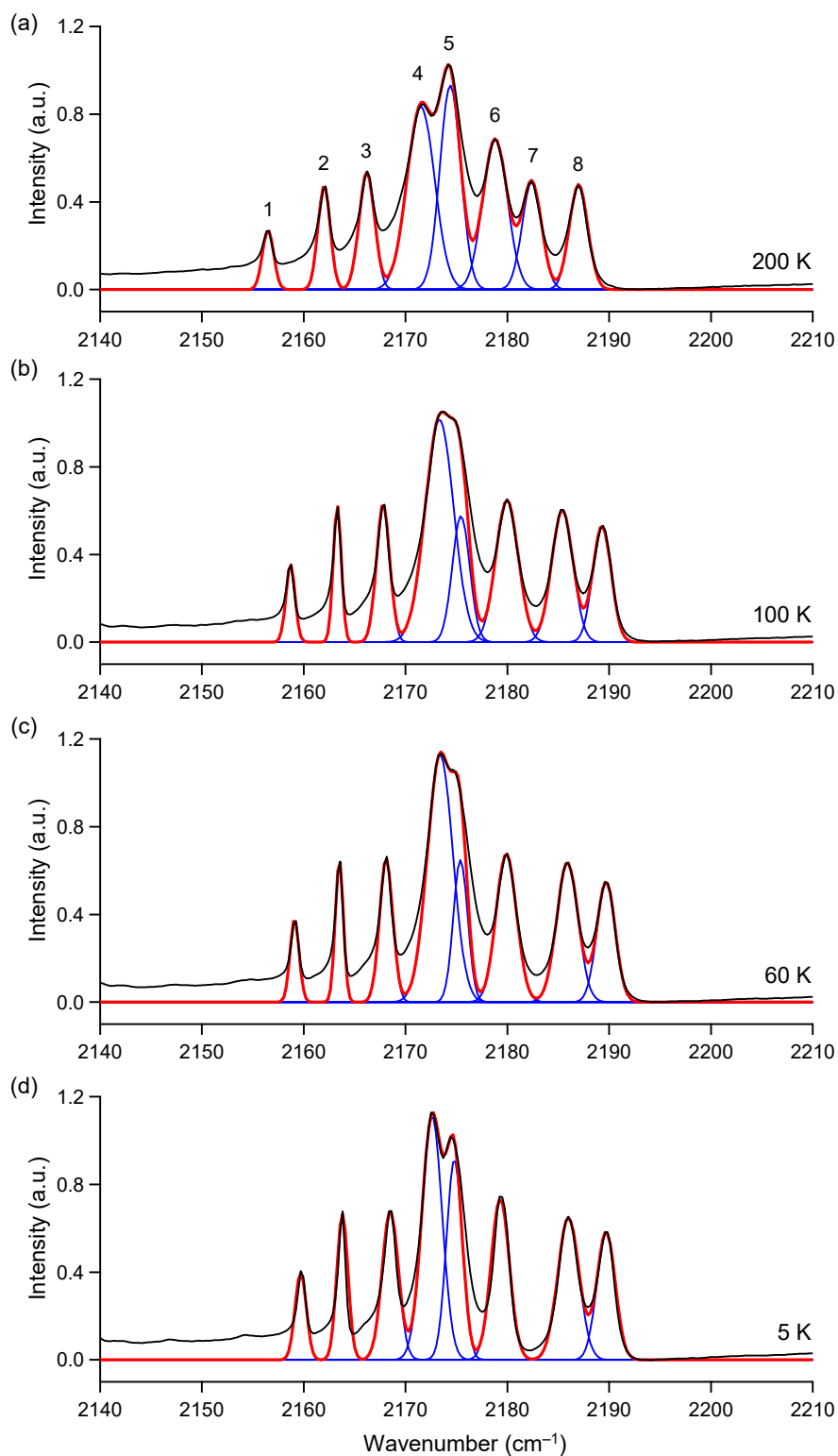


Figure S5. IR spectra and peak separations at (a) 200 K, (b) 100 K, (c) 60 K, and (d) 5 K. Experimentally observed spectra (black), separated peaks calculated using a Gaussian function (blue), and the sum of the separated peaks (red).

§ 7. Phonon dispersion obtained by first-principles phonon mode calculations.

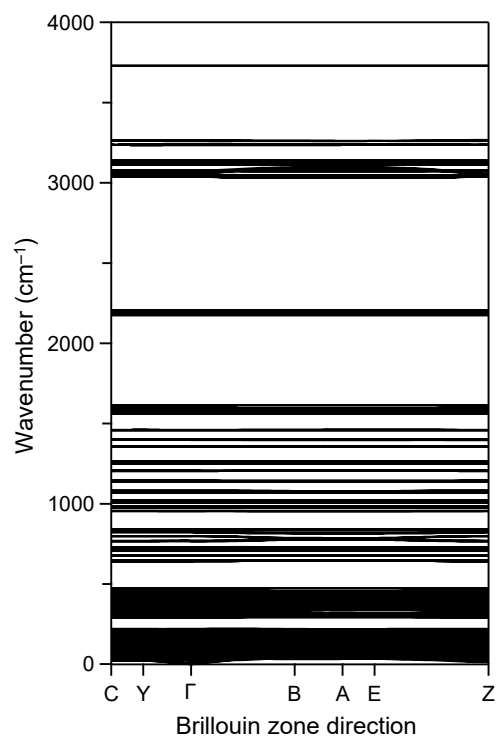
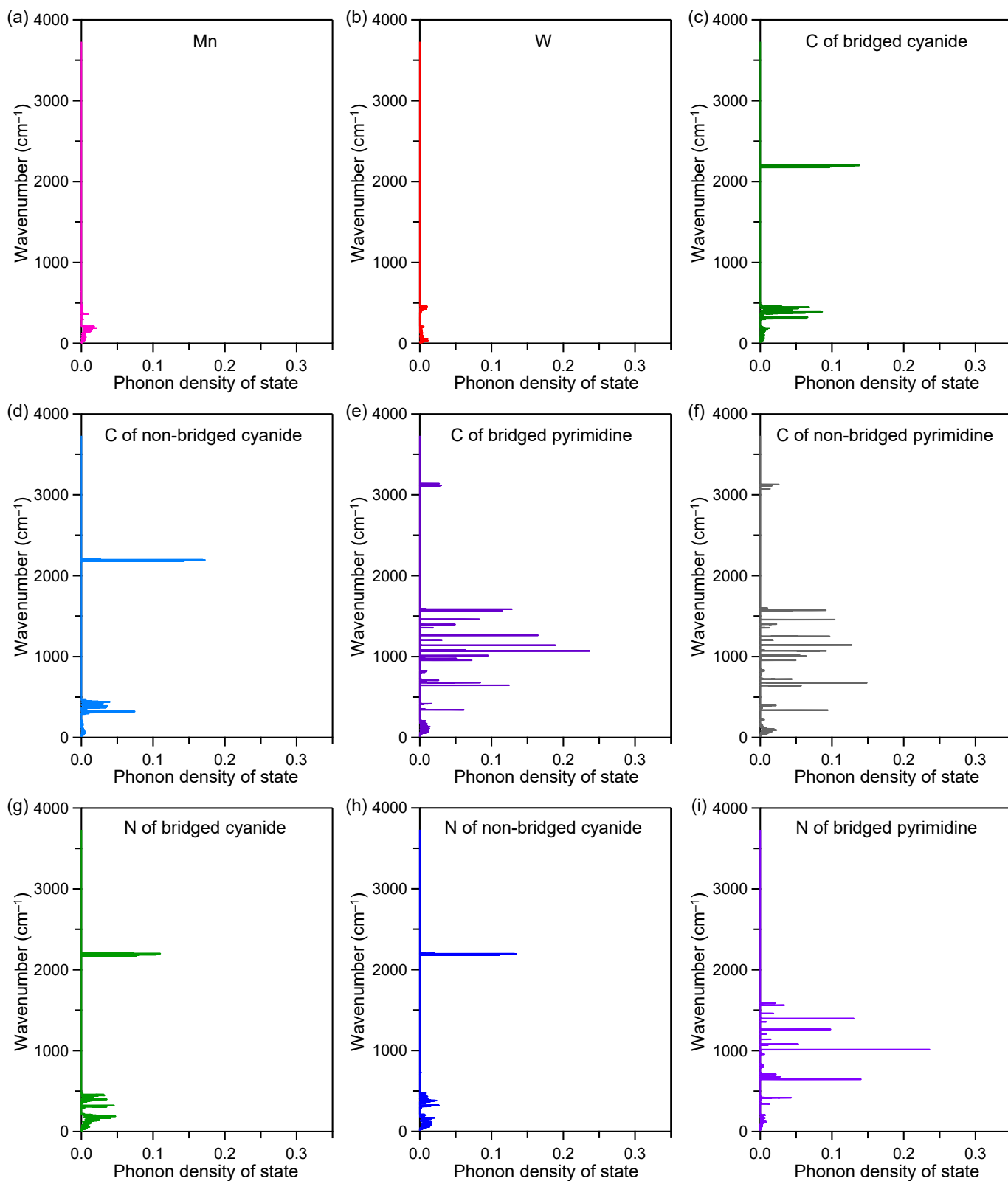


Figure S6. Phonon dispersion of **MnW** obtained by first-principles phonon mode calculations.

§ 8. Partial phonon density of states obtained by first-principles phonon mode calculations.



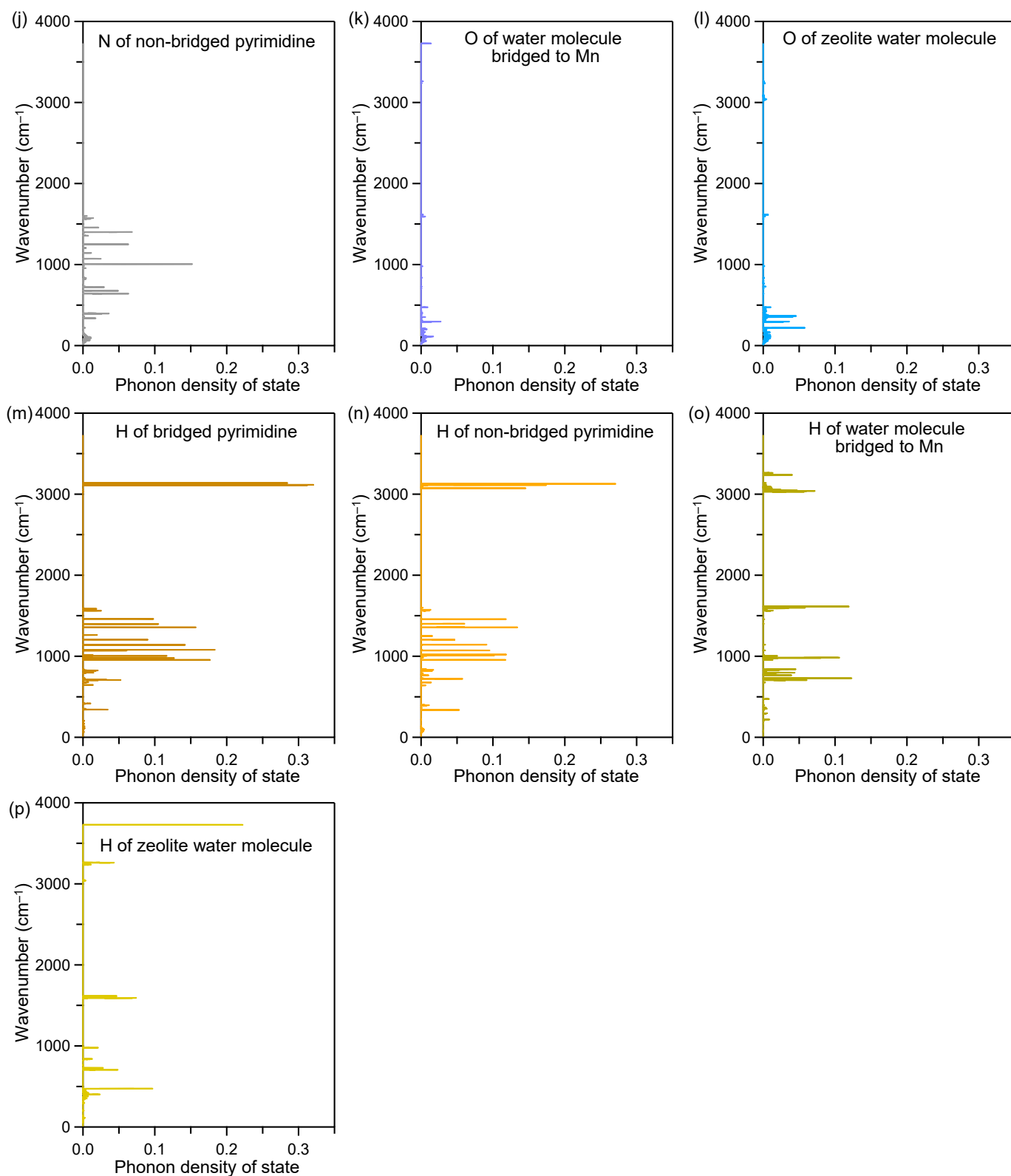


Figure S7. Partial phonon density of states (DOS) of **MnW** obtained by first-principles phonon mode calculations. (a) Mn (pink), (b) W (red), (c) C of bridged cyanide (dark green), (d) C of non-bridged cyanide (light blue), (e) C of bridged pyrimidine (dark purple), (f) C of non-bridged pyrimidine (dark grey), (g) N of bridged cyanide (green), (h) N of non-bridged cyanide (blue), (i) N of bridged pyrimidine (purple), (j) N of non-bridged pyrimidine (grey), (k) O of water molecule bridged to Mn (dark purple), (l) O of zeolite water molecule (aqua), (m) H of bridged pyrimidine (dark orange), (n) H of non-bridged pyrimidine (orange), (o) H of water molecule bridged to Mn (dark yellow), and (p) H of zeolite water molecule (yellow).

§ 9. Far-IR spectra at 12 K and 60 K.

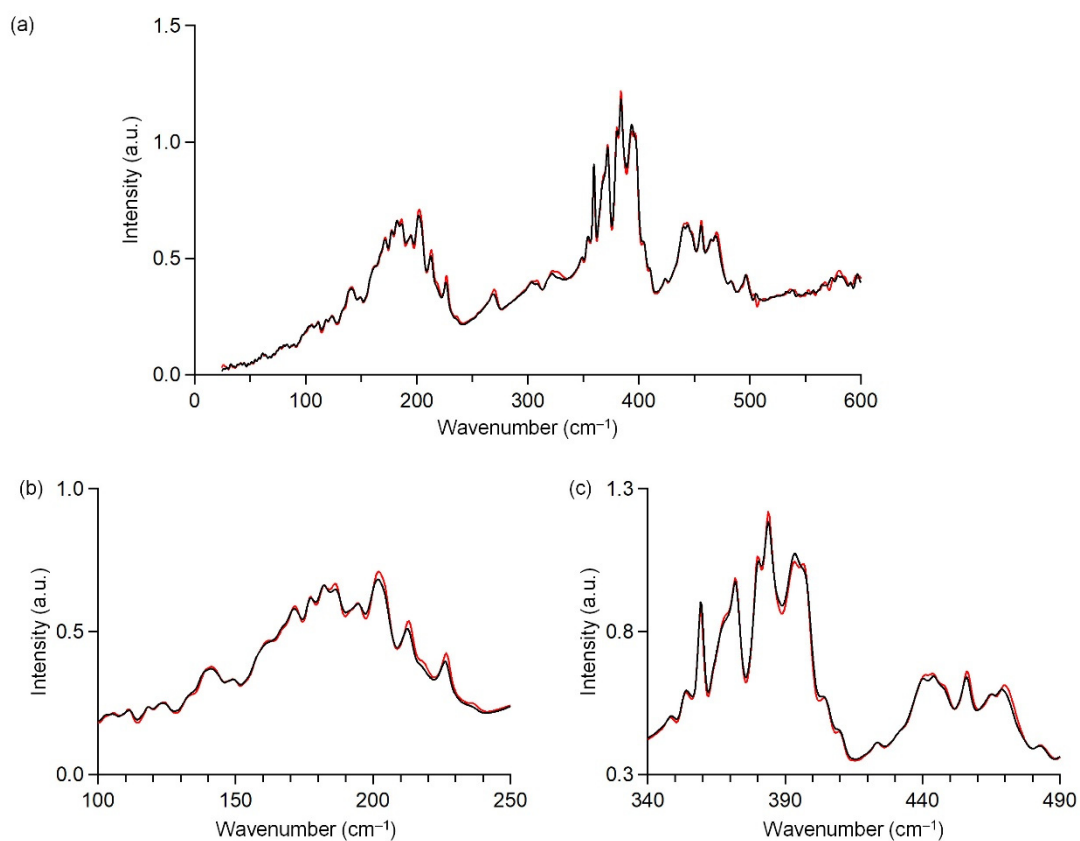


Figure S8. (a) Far-IR spectra of **MnW** at 12 K (red) and 60 K (black). (b) and (c) Enlarged views of (a) in the range of 100–250 cm⁻¹ and 340–490 cm⁻¹, respectively. Far-IR spectra at 12 K and 60 K show slight differences in the peak intensities and peak positions, which may represent the correlation between the phonon mode and long-range magnetic interaction.